

Spectral karyotyping

Yuval Garini[†], Merryn Macville[‡], Stanislas du Manoir[‡],
Robert A Buckwald[‡], Moshe Lavi[†], Nir Katzir[†], David Wine[†],
Irit Bar-Am[†], Evelin Schröck[‡], Dario Cabib[†] and
Thomas Ried^{‡§}

[†] Applied Spectral Imaging Ltd, PO Box 101, Migdal Haemek 10551, Israel

[‡] Diagnostic Development Branch, National Center for Human Genome Research,
National Institutes of Health, Bldg 49, Rm 4A28, 49 Convent Drive, Bethesda,
Maryland 20892-4470, USA

Submitted 6 August 1996, accepted 23 September 1996

Abstract. Karyotype analysis by means of chromosome banding techniques is the pillar of cytogenetic diagnostics, both in the clinical and in the cancer cytogenetic laboratory. Using chromosome banding alone, however, a disturbingly high number of chromosomal aberrations cannot be characterized comprehensively. We have therefore developed a novel karyotyping approach, termed spectral karyotyping, that is based on the simultaneous hybridization of 24 combinatorially labelled human chromosome painting probes. The visualization of all human chromosomes in different colours is achieved by spectral imaging. Spectral imaging combines fluorescence microscopy, CCD-imaging and Fourier spectroscopy to visualize, simultaneously, the entire spectrum at all image points. Here we describe the principle of spectral imaging, define software and hardware requirements, and present relevant applications of the technique to cytogenetics and cytology.

Keywords: Fourier spectroscopy, chromosome painting, karyotyping

1. Introduction

The rewarding wedlock between cytogenetics and molecular biology began when Gall and Pardue (1969) and John and colleagues (John *et al* 1969) demonstrated the possibility of localizing repetitive DNA sequences, *in situ*, with radiolabelled RNA probes. Termed *in situ* hybridization, this approach offered yet unknown flexibility for cytogenetic research and diagnostics. Being time consuming and limited to a single, isotopic detection format in the early days, the technique of *in situ* hybridization experienced an important technical improvement with the development of multiple non-isotopic labelling and fluorescence detection formats. Due to progress in methodology, the spectrum of applications of fluorescence *in situ* hybridization, equally well known under the acronym FISH, has broadened considerably and FISH has become an important molecular cytogenic technique that bridges the methodological gap existing between chromosome banding studies, on the one hand, and molecular biology techniques, on the other, both with respect to problems in basic research and medical genetic diagnostics.

One of the most attractive features of FISH is the possibility to simultaneously visualize multiple targets in different colours. Multicolour FISH offers the possibility to include internal hybridization controls, and it facilitates the comprehensive analysis of clinical samples that are in short supply and not easily retrievable. Serious attempts to increase the numbers of discernible fluorescence probes were initiated by Nederlof and colleagues in 1989 using centromere specific DNA probes that were labelled with three different fluorochromes (Nederlof *et al* 1989): AMCA (blue fluorescence), FITC (green fluorescence) and rhodamine (red fluorescence). The colour discrimination was based on the use of fluorochrome specific optical filters. The same group reported in 1990 that the number of discernible target regions can be greater than the numbers of fluorochromes (Nederlof *et al* 1990). This was achieved by a combinatorial labelling strategy, in which one DNA probe was not only labelled with a pure fluorochrome but also with a combination of two. This strategy was extended by using combinatorial fluorescence in conjunction with digital imaging microscopy to simultaneously distinguish up to seven centromere specific repeat clones, whole chromosome painting probes and locus specific cosmid clones (Ried *et al* 1992a). In the same year, Dauwerse *et al*

§ Author to whom correspondence should be addressed. E-mail address: tried@nchgr.nih.gov

(1992) reported the use of a multi-bandpass filter and ratio-labelling to discern up to 12 chromosome painting probes. The potential of using directly conjugated fluorescence nucleotides was described by Wiegant *et al* (1993) and the application of multicolour FISH to diagnostically relevant problems was explored (see, e.g., Ried *et al* 1992b,c). However, the routine use of multicolour FISH in the clinical laboratory still awaits realization (Ledbetter 1992), which is mainly due to technical difficulties in multicolour FISH imaging. There are limited numbers of spectrally separated dyes, and such problems as precise image registration need to be addressed. Because of these difficulties, distinguishing 24 combinatorial labelled targets (the number of human chromosomes) by filter-based methodology could not be achieved until recently (Speicher *et al* 1996). It became possible with the use of multiple exposures through single band-pass filter sets for image acquisition followed by software-based image registration and data analysis.

Here we describe a novel imaging technique for the analysis of FISH experiments (Schröck *et al* 1996). The approach is termed spectral karyotyping (SKY) and is based on spectral imaging (Malik *et al* 1996, Garini *et al* 1996). Spectral imaging, as the terminology suggests, combines spectroscopy and imaging. In dramatic contrast to conventional epifluorescence microscopy in which fluorochrome discrimination is based on the measurement of a single intensity through a fluorochrome specific optical filter, spectral imaging allows one to measure and analyse the full spectrum of light at all pixels of the image. We will specify hardware and software requirements for spectral karyotyping, present relevant examples of SKY analysis and discuss future applications of spectral imaging for chromosome research and cytogenetic and cytological diagnostics.

2. The spectral imaging system

2.1. General structure and performance

Figure 1 shows a diagram of a spectral imaging system. The light emitted from each point of the sample is collected with the microscope objective and sent to a collimating lens (the system can also be attached to any other optics such as a telescope or a simple lens). The collimated light travels through a Sagnac interferometer and is focused on a charged coupled device (CCD). The data are collected and processed with a personal computer. The heart of a spectral imaging system consists of an optical dispersion element that allows measurement of the full spectrum for each pixel (Malik *et al* 1996).

Here we describe the SD 200 spectral imaging system SpectraCube. The approach described here is based on Fourier spectroscopy (Bell 1972). This method offers several advantages compared to other methods for spectral imaging, such as acousto-optical tunable filters. Most importantly, the spectral imaging system has a high optical

throughput, high (and variable) spectral resolution, a broad spectral bandwidth and it is independent of polarization. The detector used in the SD 200 system is a high-performance 512×512 pixels, 12 bits cooled CCD camera (Princeton Instruments, ST-138) with a pixel size of $16 \times 16 \mu\text{m}^2$. The spatial resolution of the system is related to the pixel size according to the Nyquist sampling theorem as follows:

$$X_{\min} = \frac{2D}{M} \approx \frac{2 \times 16}{100} = 0.32 \mu\text{m} \quad (1)$$

where X_{\min} is the smallest separable feature, D is the pixel size and M is the microscope magnification being used (in this example, $\times 100$).

2.2. Principle of Fourier spectroscopy

An interferometer forms the heart of a Fourier-based spectrometer. The interferometer divides the incoming beam (in this case, the light projected from the microscope) into two coherent beams and creates a variable optical path difference (OPD) between them. The beams are then recombined to interfere with each other, and the resulting interference intensity is measured by the detector as a function of the OPD. The intensity against OPD function is called an interferogram. The subsequent Fourier transformation of the interferogram recovers the spectrum. We will now describe the Fourier transformation in more detail.

A monochromatic light at wavelength λ_0 can be described in terms of the electric field, $E(\sigma_0)$, as follows:

$$E(\sigma_0) = A(\sigma_0) \cos(2\pi\sigma_0x - \omega t). \quad (2)$$

Here σ_0 is the wavenumber of the monochromatic light in units of cm^{-1} , where $\sigma_0 = 1/\lambda_0$ (the wavenumber is the preferred unit for Fourier spectroscopy), $A(\sigma_0)$ is the amplitude of the monochromatic light of wavenumber σ_0 and ω is the angular frequency (in radians s^{-1}) of the travelling wave ($\omega = 2\pi c/\lambda = 2\pi c\sigma$, where c is the speed of light). The intensity of the monochromatic light, $I(\sigma_0)$, is equal to its amplitude squared, $[A(\sigma_0)]^2$, while x is the axis of incidence of the wave and t is the time (for simplicity it is assumed that the light is linearly polarized parallel to the z -axis).

A non-monochromatic light beam can be expressed as an integral over many monochromatic components,

$$E = \int A(\sigma) \cos(2\pi\sigma x - \omega t) d\sigma. \quad (3)$$

The total intensity of this source is given by $I = \int A^2(\sigma) d\sigma$.

Using this equation, it can be shown that for a beam that enters the interferometer which is delayed by an OPD

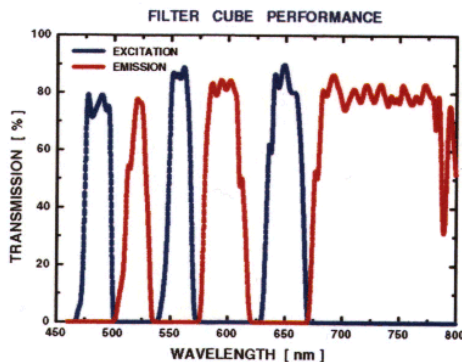
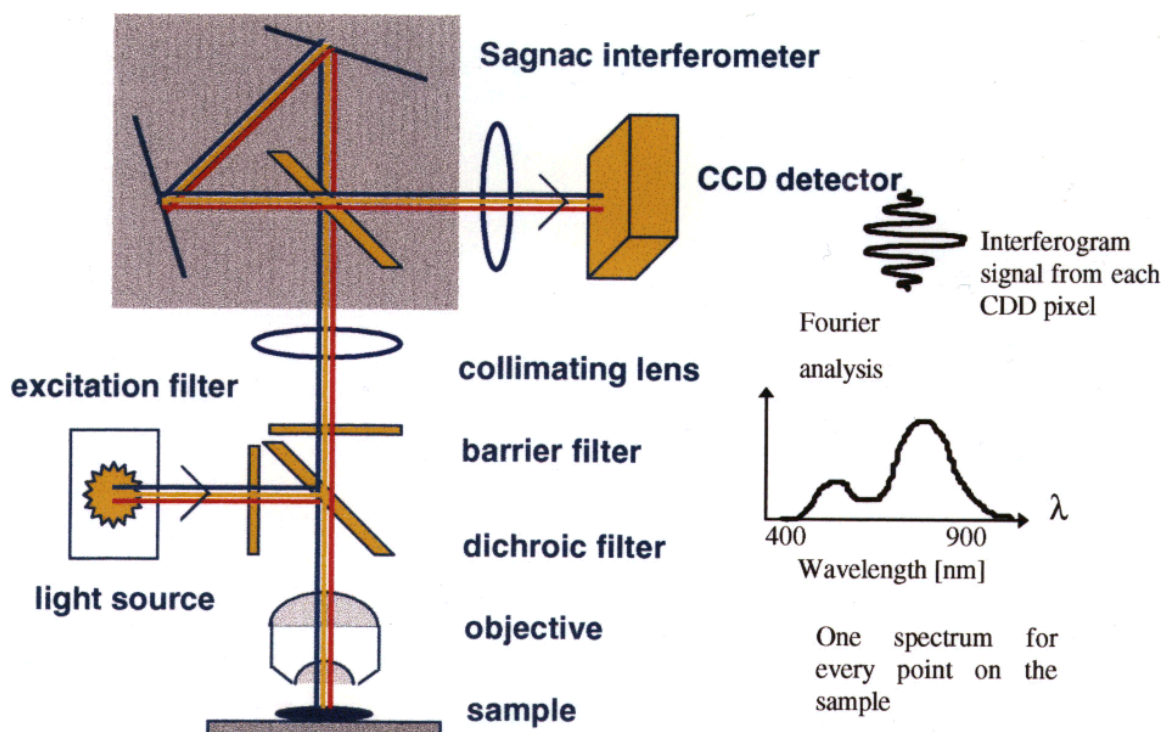


Figure 1. Diagram of the spectral imaging system that is connected to a conventional epifluorescence microscope. The light emitted by the object is collimated in the front lens and sent to the Sagnac interferometer. The interferometer generates a variable optical path difference (OPD). This OPD is computer controlled and can thus be changed. The light leaving the interferometer is focused on a pixel of a CCD camera. The repeated measurements with distinctly changed OPDs allow one to generate an interferogram for each pixel. Fourier transformation recovers the spectrum. The lower part of the figure presents the transmission curve of the custom-made triple-bandpass filter that allows all dyes to be excited and their emission spectrum measured in a single exposure.

that equals D , the intensity measured by the detector right after the interferometer, $I_{\text{det}}(D)$, is

$$I_{\text{det}}(D) = 0.5 \left[\int I(\sigma) d\sigma + \int I(\sigma) \cos(2\pi\sigma D) d\sigma \right]. \quad (4)$$

Here $I_{\text{det}}(D)$ is the interferogram, i.e. the interference intensity measured by the detector as a function of the OPD. Note that the first term of equation (4) is the total intensity of the source. This term does not depend on the OPD

and it is, therefore, a constant term in the interferogram. The second term, however, does depend on the OPD and, therefore, contains the spectral information. This second term is actually (by definition) the real part of the Fourier transform of $I(\sigma)$, i.e.

$$I_{\text{det}}(D) = c_1 + \text{Re}\{FT[I(\sigma)]\} \quad (5)$$

where c_1 is a constant. In order to measure this function, it is necessary to measure the intensity at many

points of different D . This can be done by controlling the OPD created by the interferogram which is in the Sagnac interferometer achieved by rotating the whole interferometer with respect to the incoming beam.

The reconstruction of the spectrum is based on the Fourier transformation of the measured interferogram, $I_{\text{det}}(D)$. In practice, the interferogram is a discrete function and its Fourier transform is given by

$$I(\sigma) = \Delta x \sum I(D) e^{-i2\pi\sigma D} \quad (6)$$

where $I(\sigma)$ is the spectrum of the measured light beam. In equation (6) the sum is taken over all OPD values in the scanned image.

Generally, three additional operations are performed on the interferometric data prior to Fourier transformation: (i) phase correction, (ii) apodization and (iii) zero filling. The phase correction algorithm is performed to compensate for complex terms that are introduced during the Fourier transformation. The apodization algorithm compensates for ‘edge effects’ introduced by the finite measurement taken for an infinite interferogram, and the zero filling is an optional interpolation algorithm that increases the number of data points in the spectrum. These algorithms are commonly used in Fourier spectroscopy and a detailed description can be found in Bell (1972) and Chamberlain (1979).

2.3. The SpectraCube interferometer and spectral performance

The SpectraCube system utilizes a common path Sagnac interferometer. Its optical diagram is shown in figure 1. Two beams travel in the same path, but in opposite directions. Due to its common path, the interferometer is intrinsically very stable. The OPD created by the Sagnac interferometer depends on the incidence angle of light on the beam splitter. When the beam is parallel to the interferometer axis, the OPD created will be zero. For a beam whose incidence angle relative to the optical axis is α , the OPD is given by a linear expression

$$D \cong k\alpha \quad \text{for } \alpha \ll 1 \text{ rad} \quad (7)$$

where k is a constant.

The Fourier transform theory also shows that the resolving power $R = \lambda/\Delta\lambda$ of the measurement is proportional to the maximum OPD which is scanned for the interferogram, or OPD_{max} . In our case the OPD_{max} is given by the maximum rotational angle which does not introduce vignetting. It turns out that the spectral resolution which can be obtained with the system described here is greater than 0.01λ , or 4 nm at 400 nm. (In practice, for most applications and to gain measurement time it is preferable to work with a lower spectral resolution, typically 10–15 nm at 400 nm.) A measurement with an exposure time of 400 ms for one frame and a spectral resolution

of 10 nm at 400 nm takes about 60 s. Increasing the spectral resolution increases that time linearly (i.e. 120 s for a spectral resolution of 5 nm at 400 nm).

3. Spectral karyotyping (SKY)

Spectral karyotyping refers to the application of spectral imaging to the simultaneous visualization of all human (or other species) chromosomes in different colours (Schröck *et al* 1996). To achieve this goal, 24 human chromosome specific painting libraries were labelled either singly or in combination of up to three fluorochromes and hybridized simultaneously to metaphase chromosome preparations. The fluorochromes that were used in the examples presented here include Spectrum Green, Cy3, Texas Red, Cy5 and Cy5.5.

3.1. Probe labelling, hybridization and detection

While all possible kinds of DNA probes can be used for spectral imaging, we will focus in this subsection on the use of chromosome painting probes and their application for the detection of chromosomal aberrations in clinical and cancer cytogenetics. The chromosome painting probes were generated by high-resolution and flow sorting of human chromosomes and DNA amplification using degenerate oligonucleotide primed PCR (DOP-PCR) (Telenius *et al* 1992). The chromosome specific PCR products were labelled by directly incorporating haptenized (biotin and digoxigenin) or fluorochrome (Spectrum Green, Cy3, Texas Red) conjugated nucleotides, again via PCR. Other chromosome-specific painting probes or chromosome arm or band-specific painting probes generated by microdissection can also be used (Guan *et al* 1993). The combined probe sets were ethanol precipitated in the presence of an excess of unlabelled Cot-1 DNA. This results in a suppression hybridization and, therefore, permits chromosome specificity. Hybridization conditions are not different from any other FISH experiment. Chromosome painting probes that were labelled with direct fluorochrome conjugates did not require secondary detection steps. Biotin and digoxigenin labelled probes were detected with avidin Cy5 and anti-dig Cy5.5, respectively. Chromosomes were counterstained with DAPI and embedded in an antifade solution.

The multicolour hybridizations were visualized using the SD200 SpectraCube system mounted on a Leica DMRBE microscope equipped for epifluorescence. The use of a custom-designed triple band-pass filter (figure 1) allows all dyes to be excited in a single exposure. Broad emission windows in that filter guarantee that the spectrum of the emission light can be measured without changing the filter. The filter specifications are described in Schröck *et al* (1996). The normalized spectra measured with this filter cube are shown in figure 2.

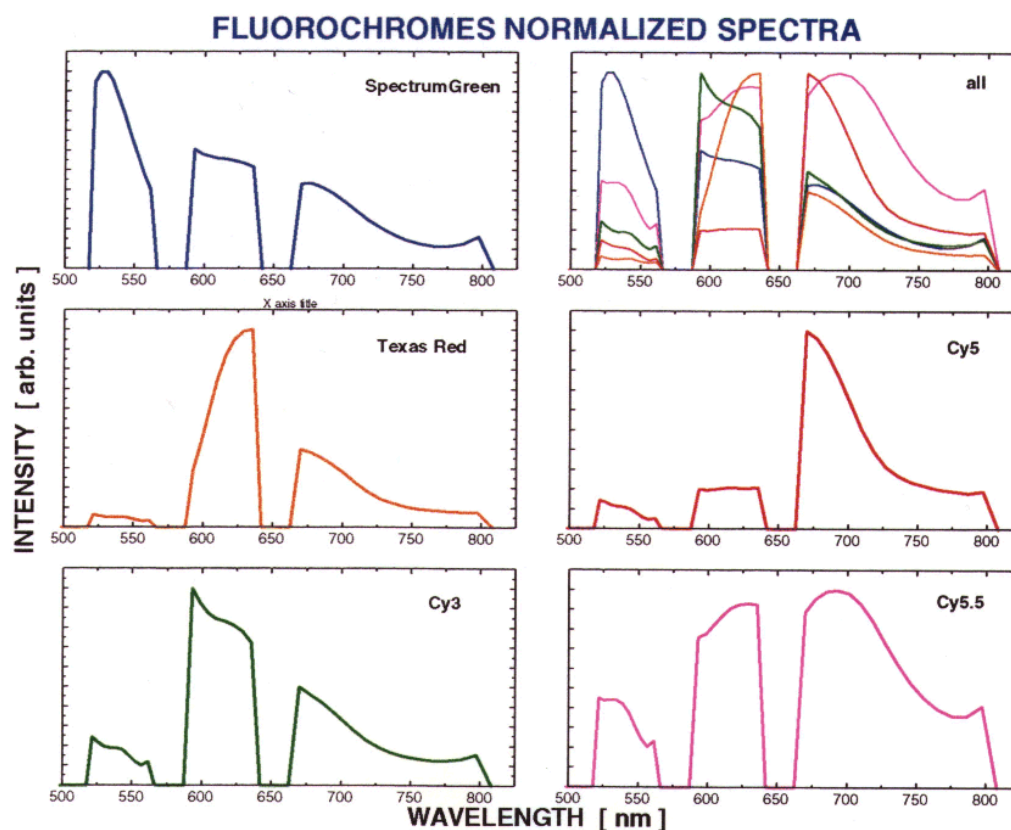


Figure 2. The spectra measured for the five fluorochromes. The spectra shown are normalized by dividing each spectrum by the transmission spectrum (of the emission band) of the triple-bandpass filter. Note the degree of overlap of the different spectra. However, the spectral shape difference is still large enough to enable the identification of all the 24 different combinations after measuring the spectral image.

The spectral measurements of the hybridization were first displayed by assigning a red, blue and green (RGB) look-up table to specific sections of the emission spectrum (figures 3(A) and (C)). For instance, chromosome 20, labelled only with Spectrum Green appears blue, chromosome 4 (Cy3 and Texas Red) appears green and chromosome 2 (Cy5) appears red. The RGB display allows the assessment of important parameters of the hybridization, for example intensity and homogeneity (figures 3(A) and (C)). However, a definitive colour separation can be achieved only by spectral classification (figures 3(B) and (D)). The spectra-based classification also forms the basis for the karyotype analysis. The algorithms that are used for this purpose are, therefore, described in detail in the following subsection.

3.2. SKY analysis

The spectral image measured by the system, $I_{x,y}(\lambda)$, is analysed by algorithms that were specifically developed for the automated classification of all chromosomes according to the spectrum.

The spectrum-based classification algorithm can be summarized in the following steps.

(1) A spectral library is built that holds the spectrum of each chromosome, as measured in an independently identified metaphase.

(2) All the spectra of the measurement including the reference spectra are normalized to an area that equals 1.

(3) For each pixel x, y in the image the Euclidean distance, d_i , between its measured spectrum, $I_{x,y}(\lambda)$, and each of the reference spectra, $I_i(\lambda)$, (class $i = 1, 2, \dots, 24$ in our case, one for each chromosome) is calculated:

$$d_{x,y,i} = \left(\int (I_{x,y}(\lambda) - I_i(\lambda))^2 d\lambda \right)^{1/2}. \quad (8)$$

The integration is performed over the spectral range covered by the emission spectra of all fluorochromes. A smaller distance means a higher degree of similarity.

(4) Select the reference spectrum $I_i(\lambda)$ for which d_i is the smallest. This class i is chosen as the one to which the pixel's spectrum $I_{x,y}(\lambda)$ is most similar, and the pixel is assigned to chromosome I .

(5) A classification colour is assigned to the emission spectrum specific for each chromosome, for example yellow

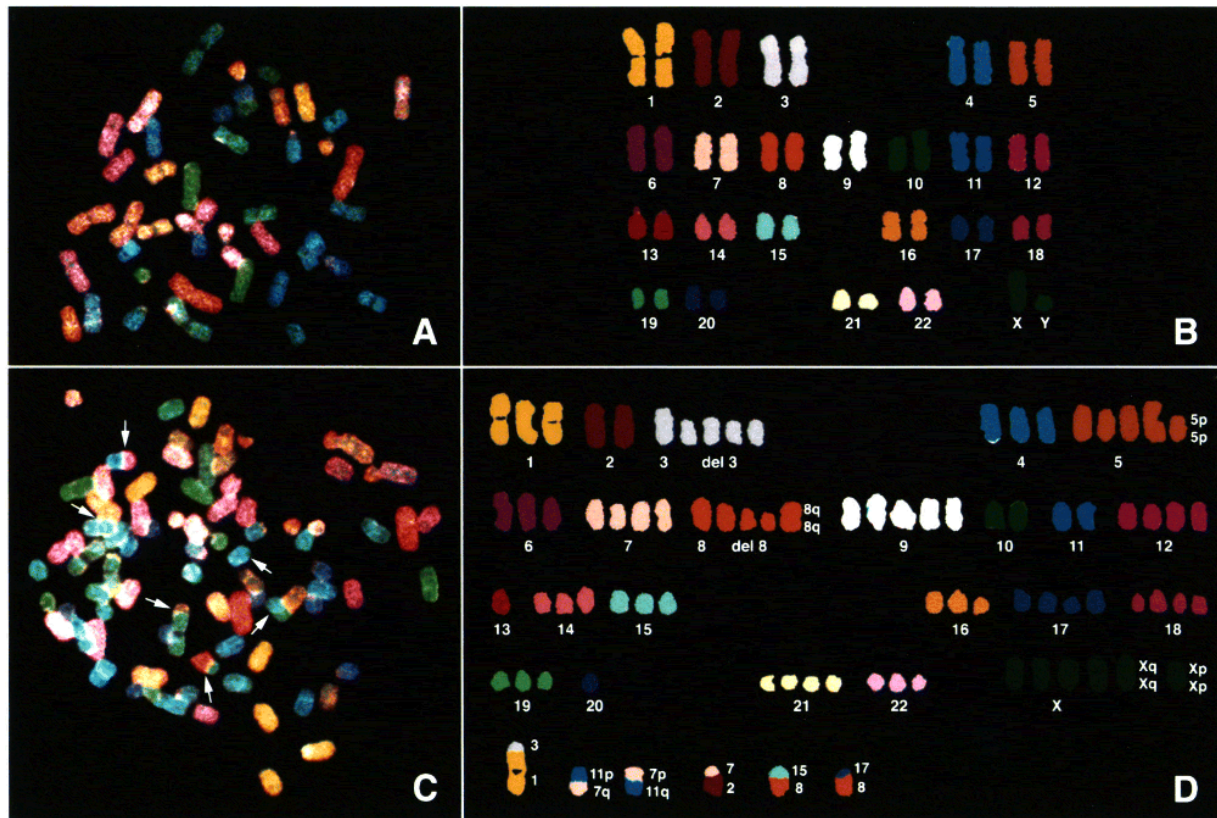


Figure 3. SKY on human chromosomes. (A) SKY was applied with a probe set of 24 differentially labelled human chromosome painting probes to normal human chromosomes provided by a male donor. The hybridization was visualized by assigning a RGB look-up table to defined ranges of the measured spectrum. Using this colour assignment, chromosomes that were labelled with similar fluorochromes appear in similar colours. (B) Spectra-based classification of the metaphase shown in (A). The classification allows one to karyotype the human chromosome complement. Each pixel with the same spectrum was assigned the same classification colour. (C) Hybridization of 24 human chromosome-specific probes to metaphase chromosome prepared from a cervical carcinoma cell line (SW756). The RGB look-up table allows one to immediately assess the entire chromosome complement. (D) Spectra-based karyotyping of the metaphase shown in (C). All of the marker chromosomes could be readily identified. Multiple aberrant chromosomes and numerous chromosomal translocations (bottom line) define this particular cell line.

for chromosome one, brown for chromosome two, etc. A colour image is then created in which every pixel is displayed in the colour that corresponds to the chromosome specific emission spectrum to which that colour was assigned.

4. Results and applications

Measuring the full spectrum for each pixel has major advantages over measurements of one or few grey-level images through narrow band-width filters. The most important advantages are as follows.

- Emission spectra of all fluorochromes are measured in a single exposure. Consequently, image registration problems do not exist, and all information is contained in one spectral image.

- Distinction of fluorochromes with overlapping emission spectra occurs even if spectral shifts are subtle.

- The analysis is not based on absolute intensities and therefore not sensitive to changes of the intensity of one or few of the fluorochromes. Although this information exists in the spectral image, the analysis is based only on differences in spectral shapes of the different fluorochromes. This feature is clearly documented in figure 4. Notable changes in the intensity of the cytoplasmatic autofluorescence do not affect the spectral classification.

- The measurement of the entire spectrum allows one to readily change a set of dyes. This provides flexibility to integrate new fluorescence dyes.

- Background fluorescence can be precisely measured and, therefore, subtracted. This increases the accuracy of fluorochrome (and therefore chromosome) identification.

- Autofluorescence of biological structures can be identified and subtracted, because, in general, the spectrum should be different from the signal's spectrum.

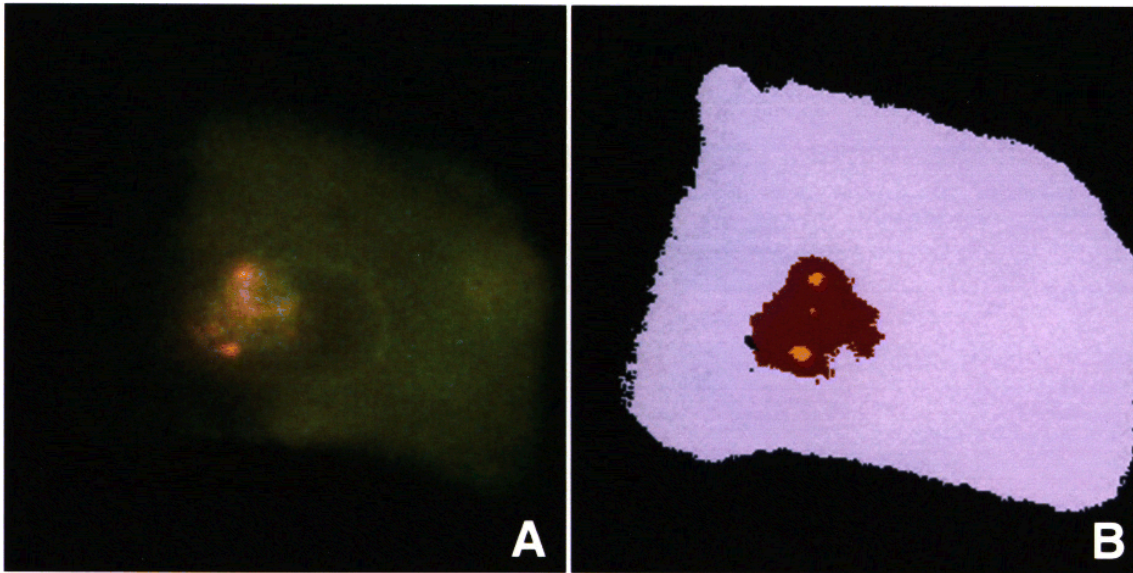


Figure 4. Interphase FISH using a centromere specific repeat clone for chromosome 3 labelled with rhodamine. (A) The hybridization was performed directly on routine cytological preparations (PAP-smears) and visualized through a FITC longpass filter (Leica N1). Note that a considerable degree of background fluorescence occurs in the nucleus as well as in the cytoplasm. (B) The spectra-based classification algorithm was applied to this preparation. The results show that the spectra of cytoplasm, nucleus and the signals are distinctly different from one another and can, therefore, be unambiguously identified. The small spot between the hybridization signals for the chromosome 3 probe reflects few background pixels with the same spectrum as the probe signals.

Figure 3 presents examples of SKY of normal and aberrant human metaphase chromosomes. The hybridization of the metaphase spreads are presented after assigning a RGB look-up table to different ranges of the spectrum (figures 3(A) and (C)). This display allows the assessment of important parameters of a FISH experiment, such as the homogeneity of the hybridization. Based on the spectral classification of the chromosome-specific emission spectra, a karyotype analysis can be performed (figures 3(B) and (D)). This allows the unambiguous identification of all human chromosomes in classification colours that depend solely on the measured spectrum (and are not dependent on intensities). One obvious application of SKY relates to the analysis of complex chromosomal re-arrangements in solid tumour cytogenetics. As an example of the potential of SKY to elucidate highly re-arranged karyotypes we have analysed metaphase chromosome preparations from a cervical carcinoma cell line, SW756 (figure 3(C) and (D)). Again, the hybridization to the metaphase is presented using a RGB look-up table. However, the spectra-based classification allows the unambiguous identification of all chromosomes after a single measurement of about 60–90 s. Many of these aberrations were not described before by chromosome banding alone.

The use of SKY to study constitutional chromosome abnormalities is particularly useful for identifying *de novo* balanced and unbalanced translocations, which are occasionally quite small and difficult to identify; it is imperative that the chromosomal origin of these

markers can be determined since some of them have considerable prognostic significance (e.g., those derived from chromosome 18) while others appear to have less clinical consequences. SKY can quickly identify the source of minute markers. It is clear, however, that SKY using the chromosome painting probe will have its major advantage in identifying interchromosomal aberrations. Paracentric inversions or pericentric inversions that do not affect the shape and the length of the chromosomes, as well as submicroscopic deletions, will remain difficult to identify using painting probes alone. It is perceivable that future probe sets will become specifically tailored for these diagnostic needs.

SKY will also have great potential use in comparative cytogenetics, i.e. in the study of chromosomal re-arrangement that occurred during the course of chromosome evolution (Wienberg *et al* 1990).

Another application of SKY will extend to the multiparameter analysis of cytological preparations. An example of the application of spectral imaging to routine diagnostic preparations is shown in figure 4. Using interphase FISH, a cell from a cervical PAP-smear preparations was hybridized with a DNA probe that recognized the centromere of chromosome 3. The image, as it appears through a conventional optical filter, is shown in figure 4(A). Note the intense autofluorescence and background staining throughout the cell. This cell was subjected to spectral imaging and a subsequent spectral classification, meaning that all pixels in the image that

have the same spectrum have the same classification colours. The spectral classification allows the unambiguous discernment between the signal, the fluorescence of the cell nucleus and the apparent autofluorescence of the cytoplasm (figure 4(B)).

In the short term of the application of spectral imaging to cytogenetic research and diagnostics, it has become clear that the advantages of SKY might help to automate karyotype analysis, greatly facilitate the analysis of complex chromosomal re-arrangements that define solid tumours and aid considerably the analysis of cytological preparations, by allowing an accurate spectral classification of signal against background fluorescence.

Acknowledgments

The authors are indebted to Drs Nicholas Popescu and Drazen Zímonjic for providing the cervix carcinoma cell line, Dr Keerti Shah for providing the PAP-smear specimen and Drs Malcolm A Ferguson-Smith and Johannes Wienberg for providing the flow-sorted painting probes. ES received a stipend from the Deutsche Forschungsgemeinschaft. The continuous support of Dirk Soenksen is gratefully acknowledged.

References

- Bell R J 1972 *Introductory Fourier Transform Spectroscopy* (London: Academic)
- Chamberlain J E 1979 *The Principles of Interferometric Spectroscopy* (New York: Wiley)
- Dauwerse J G, Wiegant J, Raap A K, Breuning M H and van Ommen G J B 1992 Multiple colors by fluorescence in situ hybridization using ratio-labelled DNA probes create a molecular karyotype *Hum. Mol. Genet.* **1** 593–8
- Gall J G and Pardue M L 1969 Formation and detection of RNA-DNA hybrid molecules in cytological preparations *Proc. Natl Acad. Sci., USA* **63** 378–83
- Garini Y, Katzir N, Cabib D, Buckwald R A, Soenksen D and Malik Z 1996 Spectral bio-imaging *Fluorescence Imaging Spectroscopy and Microscopy* ed X F Wang and B Herman (New York: Wiley)
- Guan X-Y, Trent J M and Meltzer P S 1993 Generation of band-specific painting probes from a single microdissected chromosome *Hum. Mol. Genet.* **2** 1117–21
- John H, Birnstiel M L and Jones K W 1969 RNA-DNA hybrids at cytological levels *Nature* **223** 582–7
- Ledbetter D H 1992 The ‘colorizing’ of cytogenetics: is it ready for prime time? *Hum. Mol. Genet.* **1** 297–9
- Malik Z, Cabib D, Buckwald R A, Talmi A, Garini Y and Lipson S G 1996 Fourier transform multipixel spectroscopy for quantitative cytology *J. Microsc.* **182** 133–40
- Nederlof P M, Robinson D, Abuknesha R, Wiegant J, Hopman A S H N, Tanke H J and Raap A K 1989 Three color fluorescence in situ hybridization for the simultaneous detection of multiple nucleic acid sequences *Cytometry* **10** 20–7
- Nederlof P, van der Flier S, Wiegant J, Raap A K, Tanke H J, Ploem J S and van der Ploeg M 1990 Multiple fluorescence in situ hybridization *Cytometry* **11** 126–31
- Ried T, Baldini A, Rand T C and Ward D C 1992a Simultaneous visualization of seven different DNA probes using combinatorial fluorescence and digital imaging microscopy *Proc. Natl Acad. Sci., USA* **89** 1388–92
- Ried T, Landes G, Dackowski W, Klingner K and Ward D C 1992b Multicolor fluorescence in situ hybridization for the simultaneous detection of probe sets for chromosomes 13, 18, 21, X and Y in uncultured amniotic fluid cells *Hum. Mol. Genet.* **1** 307–13
- Ried T, Lengauer C, Cremer T, Wiegant J, Raap A K, van der Ploeg M, Groitl P and Lipp M 1992c Specific metaphase and interphase detection of the breakpoint region in 8q24 of Burkitt lymphoma cells by triple-color fluorescence in situ hybridization *Genes Chrom. Cancer* **4** 69–74
- Schröck E *et al* 1996 Multicolor spectral karyotyping of human chromosomes *Science* **273** 494–7
- Speicher M R, Ballard S G and Ward D C 1996 Karyotyping human chromosome by combinatorial multi-fluor FISH *Nat. Genet.* **12** 368–75
- Telenius H, Pelmeur A H, Tunnacliffe A, Carter N P, Behmel A, Ferguson-Smith M A, Nordenskjöld M, Pfragner R and Ponder B A J 1992 Cytogenic analysis by chromosome painting using DOP-PCR amplified flow sorted chromosomes *Genes Chrom. Cancer* **4** 263–7
- Wiegant J, Wiesmeijer C C, Hoovers J M N, Schuurin E, d’Azzo A, Vrolijk J, Tanke H J and Raap A K 1993 Multiple and sensitive fluorescence in situ hybridization with rhodamine-, fluorescein-, and coumarin labeled DNAs *Cytogenet. Cell Genet.* **62** 73–6
- Wienberg J, Jauch A, Stanyon R and Cremer T 1990 Molecular cytogenetics of primates by chromosomal in situ suppression hybridization *Genomics* **8** 347–50